ELSEVIER

Polymer 41 (2000) 7803–7814

polymer

Influence of temperature and chain orientation on the crystallization of poly(ethylene terephthalate) during fast drawing

A. Mahendrasingam[a,*], D.J. Blundell[a,b], C. Martin[a], W. Fuller[a], D.H. MacKerron[c], J.L. Harvie[c], R.J. Oldman[b], C. Riekel[d]

[a]*Department of Physics, Keele University, Staffordshire ST5 5BG, UK*
[b]*ICI Technology, P.O. Box 90, Wilton, Middlesbrough, Cleveland TS90 8JE, UK*
[c]*DuPont UK Ltd, P.O. Box 2002, Wilton, Middlesbrough, Cleveland TS90 8JF, UK*
[d]*ESRF, BP 220, F-38043 Grenoble Cedex, France*

Received 28 July 1999; received in revised form 16 December 1999; accepted 14 February 2000

Abstract

Three regimes of poly(ethylene terephthalate) (PET) deformation are identified from a detailed analysis of time-resolved wide angle X-ray scattering (WAXS) data recorded during the mechanical deformation of PET at a wide range of draw rates (0.05–12 s^{-1}), temperatures (90–120°C) and draw ratios. These are:

(i) where the onset of crystallization occurs after the end of deformation with a tendency for preferred alignment of the (100) plane in the plane of the sample;

(ii) where the onset of crystallization occurs during deformation and with increasing tilt of the crystal chain axis away from the draw direction; and

(iii) where there is no oriented crystallization.

A comparison of the crystallization rate with the orientation parameter $\langle P_2(\cos\theta)\rangle$ at the onset of crystallization shows a strong dependence of the crystallization rate on both temperature and molecular orientation. It is proposed that a previously observed insensitivity of crystallization rate to temperature was a consequence of fortuitous choice of drawing conditions in which the opposing effects of temperature and molecular orientation produced similar net crystallization rates. The effects of the temperature dependence have been factored out using a WLF shift factor to reveal an overall dependence of the crystallization rate on approximately the fourth power of $\langle P_2(\cos\theta)\rangle$. At high draw temperatures where the rate of the chain retraction motion is faster than the draw rate, there is a significant tilt of the crystal chain axis away from the draw direction. During the crystallization process both the degree of crystal tilt and the half-width of the crystal reflections remain essentially unaltered over the whole crystallization process.

Keywords: Poly(ethylene terephthalate); Orientation; Crystallization

1. Introduction

We have recently reported the use of synchrotron radiation to monitor the oriented crystallization process in poly(ethylene terephthalate) (PET) when it is deformed under the fast drawing conditions employed in the manufacture of polyester films and bottles [1,2]. The observations were made possible by the combination of the high brilliance of synchrotron X-ray radiation sources and new CCD camera technology. Our earlier reports showed that crystallization during fast drawing processes unexpectedly differed in behaviour from the results of previous laboratory experiments at slower drawing rates [1,2]. It was observed that the onset of the crystallization process did not occur until after the deformation stage. It was also found that the rate of crystallization was dependent on draw ratio but, surprisingly, was apparently insensitive to temperature.

A further series of synchrotron experiments have now been carried out to clarify these issues. The analysis of the two-dimensional (2D) diffraction patterns has been further developed to enable the process to be examined in greater detail. Some of the main observations have been summarised in a previous note [3]. In a separate associated paper [4] we have reported a detailed analysis of the azimuthal variation of the amorphous halo to give

* Corresponding author. Tel.: +44-1782-583312; fax: +44-1782-711093.
E-mail address: a.mahendrasingam@keele.ac.uk (A. Mahendrasingam).

0032-3861/00/$ - see front matter
PII: S0032-3861(00)00129-4

information of the segment orientation during drawing. It was shown that the discrepancy with previous laboratory data concerning the onset of crystallization can be rationalised in terms of the relation of the drawing rate to the relaxation rate of the chain retraction mechanism. If the drawing rate is faster than the chain retraction process, as in the fast drawn synchrotron observations, then crystallization is delayed until the deformation has finished. If the drawing rate is slower than chain retraction, as in lab experiments, then chains have sufficient freedom to align crystallographically and to initiate crystallization while drawing is still in progress.

In this paper we now extend the analysis of the recent synchrotron experiments to the oriented crystallization process itself. The crystallization kinetics derived from the equatorial intensity profile are compared with the azimuthal intensity profile to obtain a correlation with the degree of segment orientation in the samples at the onset point of crystallization. It will be shown that the apparent insensitivity of the crystallization rate to changes in draw temperature is the result of opposing effects of an increased segment mobility and a reduced segment orientation. If the temperature-related effects are factored out, then it is possible to extract the temperature independent behaviour that relates only to the degree of chain orientation. It will also be shown that there are changes in the orientation texture, which appear to correlate with the chain relaxation processes discussed previously.

2. Experimental

The experiments were carried out on beamline ID13 at the ESRF in Grenoble. Details of the experimental configuration are as described previously [4]. The PET samples were drawn in a purpose designed X-ray camera constructed in the Keele Physics Department workshops. Programmable stepping motors controlled the deformation of the samples. The beamline ID13 used a mirror monochromator to produce a highly collimated beam 30 μm diameter with a wavelength of 0.92 Å. Diffraction patterns were recorded using a Photonics Science CCD detector. Up to 496 frames were recorded "end to end" with exposure times of 40 ms and with essentially no dead time between successive frames.

Specimens 10 mm wide were cut from a sheet of 840 μm thick cast film of amorphous unoriented PET with a number average molecular weight of ~20,000. The specimen was mounted in the jaws of the camera with a 10 mm gauge length. A major problem with constant rate drawing experiments is that the mode of deformation of the polymer is unpredictable and depends on the drawing conditions. At lower temperatures and faster draw rates where the yield stress is higher, there is a greater tendency to localised necking so that the local draw ratio and draw rate of the portion being traversed by the X-ray beam is higher than that suggested by the separation of the clamps. Thus the local draw rate and draw ratio do not exactly correspond to the nominal values defined by the stepping motor program. Also, in some experiments a small macroscopic relaxation can occur as the stress is equilibrated through the samples and this can lead to a localised retraction at the point penetrated by the beam. Ink reference stripes were therefore drawn with a separation of 1 mm on the specimen at right angles to the draw direction to enable the local degree of extension to be deduced from the video camera image. The draw ratio at the point of the specimen penetrated by the X-ray beam was derived by combining the video image information with measurements of the integrated intensity using the procedures described previously [4].

A series of drawing experiments were carried out to cover a matrix of temperatures (90, 100, 110, 120°C) and nominal draw rates (1.5 and 12 s^{-1}). For most combinations of temperature and draw rate, several final draw ratios were obtained covering the range from the lowest limit where crystallization failed to occur to an upper limit of around 3.5:1. In order to extend the observations, a larger range of draw rates was examined at 90°C from 0.12 to 12 s^{-1}.

A crystallinity index was obtained from each frame from a radial intensity scan along the equatorial direction. The equatorial profile was fitted with two Pearson VII functions; one peak representing the (010) crystal reflection and the second broader peak representing all remaining crystalline and amorphous diffraction. The relative area of the (010) peak relative to the total area under the equatorial profile was taken as a crystallinity index. Although this index does not rigorously provide absolute crystallinity, previous comparisons with density measurements have demonstrated that the index gives reasonable estimates of the magnitude of actual crystallinity [2,4] and is a reliable measure of relative changes in crystallinity occurring during any one experiment.

Previous work [1,2] has shown that for the situation for fast drawing, where the crystallization onset is delayed until the end of the deformation stage, the main, primary component of the oriented crystallization process can be characterised by a first order transformation process of the form:

$$\frac{\psi_f - \psi}{\psi_f} = e^{-k_c t}$$

where ψ_f represents the final attained crystallinity, ψ is the crystallinity after time t and k_c is a crystallization rate parameter. A value for the rate parameter k_c can be obtained by curve fitting this functional form or from the slope of a plot of $\ln\{(\psi_f - \psi)/\psi_f\}$ versus t. For slower crystallization, more reliable estimates of k_c can be obtained from curve fitting, while the logarithm plot is more reliable when crystallization occurs more quickly within a few frames. When drawing at rates slower than the retraction relaxation rate, it has been found there are some deviations from a simple first-order transformation [4]. However, the above procedure still enables an estimate of the average crystallization

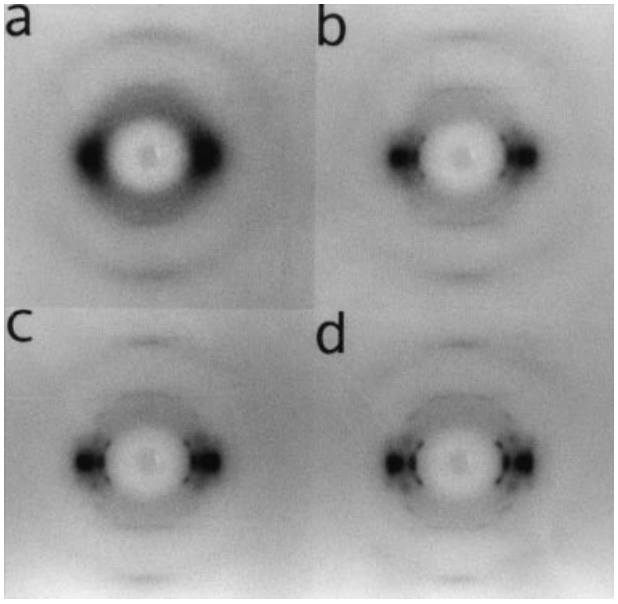

Fig. 1. Selected X-ray diffraction patterns of a PET sample drawn at 90°C, draw rate 11.5 s^{-1} and to a final draw ratio 3.5:1. Diffraction patterns (a)–(d) corresponding to frames 5 (0.20 s), 8 (0.32 s), 10 (0.40 s) and 124 (4.96 s).

rate to be derived. At longer times there is evidence of a slower, secondary crystallization process, probably associated with crystal annealing mechanisms [1].

Information on the degree of orientation of the non-crystalline structure up to and including the point of onset of crystallisation was obtained using the techniques described previously [4]. Azimuthal circular scans were made around

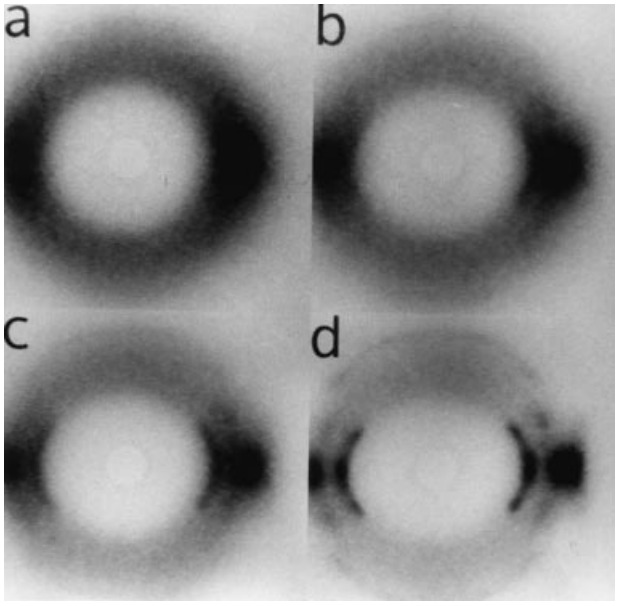

Fig. 2. Selected X-ray diffraction patterns of a PET sample drawn at 90°C, draw rate 0.56 s^{-1} and to a final draw ratio 3.8:1. Diffraction patterns (a)–(d) corresponding to frames 76 (3.04 s), 90 (3.60 s), 101 (4.04 s) and 496 (19.84 s). (In order to accommodate the 19.84 s of this experiment, the frame size was reduced from 512 × 512 to 256 × 256).

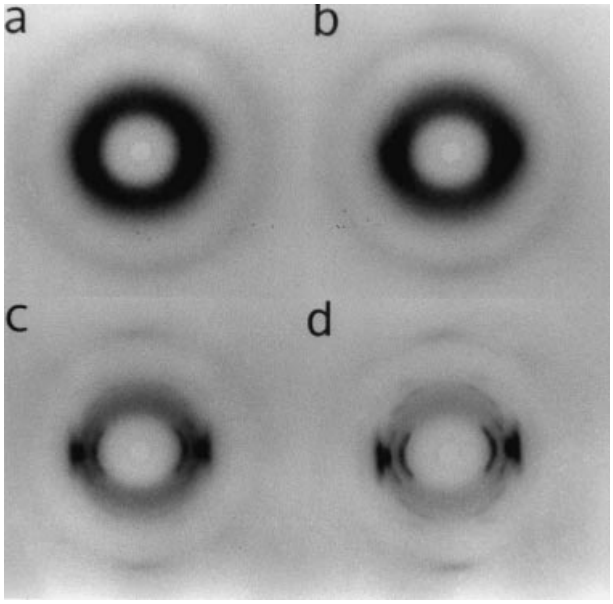

Fig. 3. Selected X-ray diffraction patterns of a PET sample drawn at 110°C, draw rate 9.9 s^{-1} and to a final draw ratio 3.8:1. Diffraction patterns (a)–(d) corresponding to frames 6 (0.24 s), 7 (0.28 s), 9 (0.36 s) and 124 (4.96 s).

the amorphous halo at the equivalent reciprocal space vector of 0.28 A^{-1}. After subtraction of a baseline, it was assumed that the azimuthal profile represented the distribution of the vectors normal to direction vectors of the segments in the non-crystalline chains. This profile was used to calculate an orientation order parameter $\langle P_2(\cos\theta)\rangle$ of the chain segments where θ is the angle between the segment direction and the draw direction. This calculation makes the simplifying assumption that the non-crystalline structure has uniaxial symmetry. The results obtained in our previous paper [4] have shown that the values of $\langle P_2(\cos\theta)\rangle$ obtained by this method are comparable with those found by other authors in similarly deformed samples. This present paper is particularly concerned with the value of $\langle P_2(\cos\theta)\rangle$ at the crystallisation onset.

3. Results

Figs. 1–4 show selected frames of diffraction patterns at various stages of deformation in four representative experiments covering various combinations of temperature and draw rate. The first frame in each set illustrates the pattern close to the onset of crystallization, where there is minimal evidence of any crystalline diffraction spots. The next three diffraction patterns in each set illustrate the development of the crystalline diffraction at various times after the onset point of crystallization. Figs. 5–8 show plots as a function of time for draw ratio and crystallinity data, which have been derived from the experiments illustrated in Figs. 1–4, respectively. Also plotted on these graphs is a fit to the first order transformation from which a value of the rate of the crystallization process can be derived.

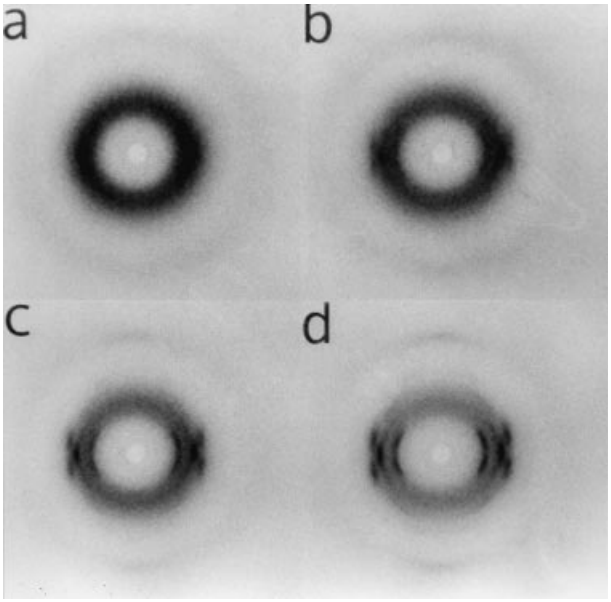

Fig. 4. Selected X-ray diffraction patterns of a PET sample drawn at 110°C, draw rate 2.1 s^{-1} and to a final draw ratio 4.6:1. Diffraction patterns (a)–(d) corresponding to frames 35 (1.40 s), 50 (2.00 s), 60 (2.40 s) and 124 (4.96 s).

For Figs. 1 and 5, the draw temperature was 90°C and the draw rate was 11.5 s^{-1} giving a final draw ratio of 3.5:1. As reported separately in our associated paper [4], the rate of drawing in this experiment is faster than the rate of relaxation due to chain retraction. It will be noted in Fig. 5 that the extrapolated onset of the crystallization closely coincides with the end of the deformation stage. The diffraction pattern at this point is in Fig. 1a, and shows only oriented amorphous diffraction with no detectable crystalline reflections. In the subsequent frames in Fig. 1b, c and d, the first prominent crystalline reflection on the equator is the (010) reflection, which is used for deriving the crystallinity index. It should be noted that the relative intensities of the crystalline reflections in the patterns of this experiment are not identical to a fibre with uniaxial symmetry. The patterns have a biaxial character due to a preference for the (100) crystal plane to align in the plane of the sample [4–7] thus reducing the strength of the (100) reflection. It is also of interest to record that samples drawn under these conditions (90°C and ~10 s^{-1}) can also exhibit a very faint, sharp meridional reflection that is not discernible with the contrast level illustrated in Fig. 1. The reflection has been associated with a transient smectic mesophase and becomes visible in the last stages of deformation and at the beginning of crystallisation; the observation has been discussed in detail in a separate publication [22].

For Figs. 2 and 6, the draw temperature is also 90°C but the draw rate is significantly slower at 0.56 s^{-1} with a draw ratio of 3.8:1. As discussed in our previous paper, this is in the regime where chain retraction can occur within the timescale of the deformation process [4]. As noted previously, the onset of crystallization is occurring well before the end

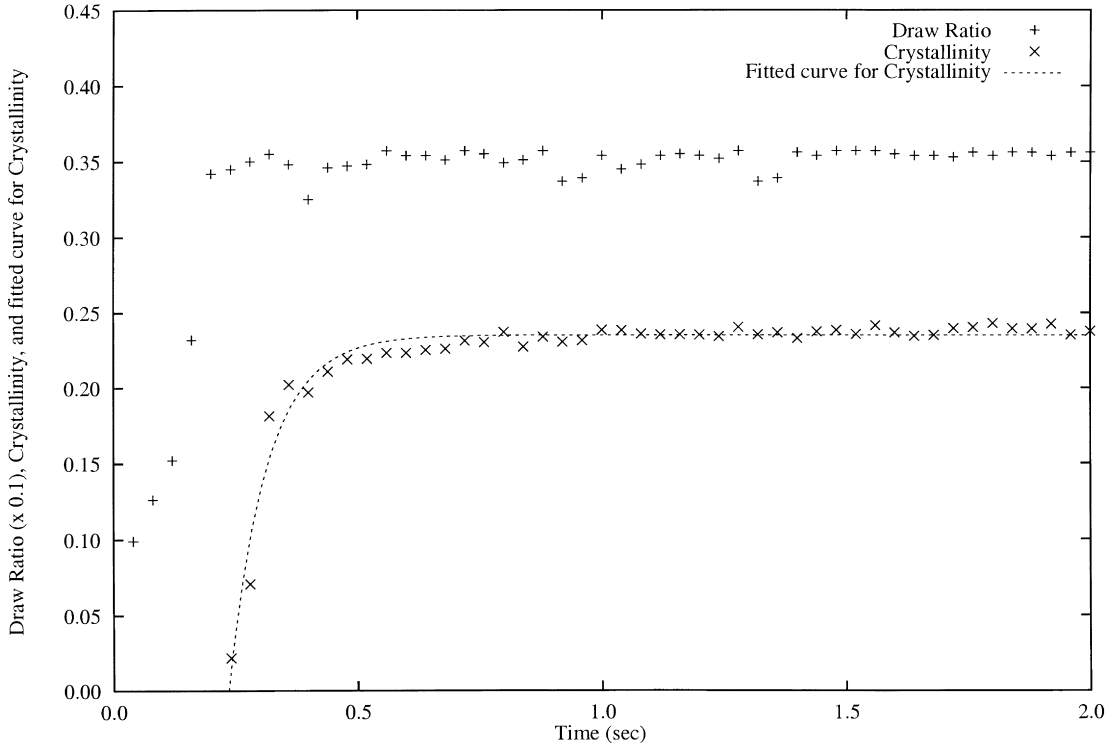

Fig. 5. Plot of the variation in draw ratio (+), crystallinity (×) calculated from the sequence of X-ray diffraction patterns of the PET sample recorded during the drawing at 90°C, draw rate 11.5 s^{-1} and to a final draw ratio 3.5:1. The dotted line indicates the fitted curve based on a first order transformation for the crystallization process.

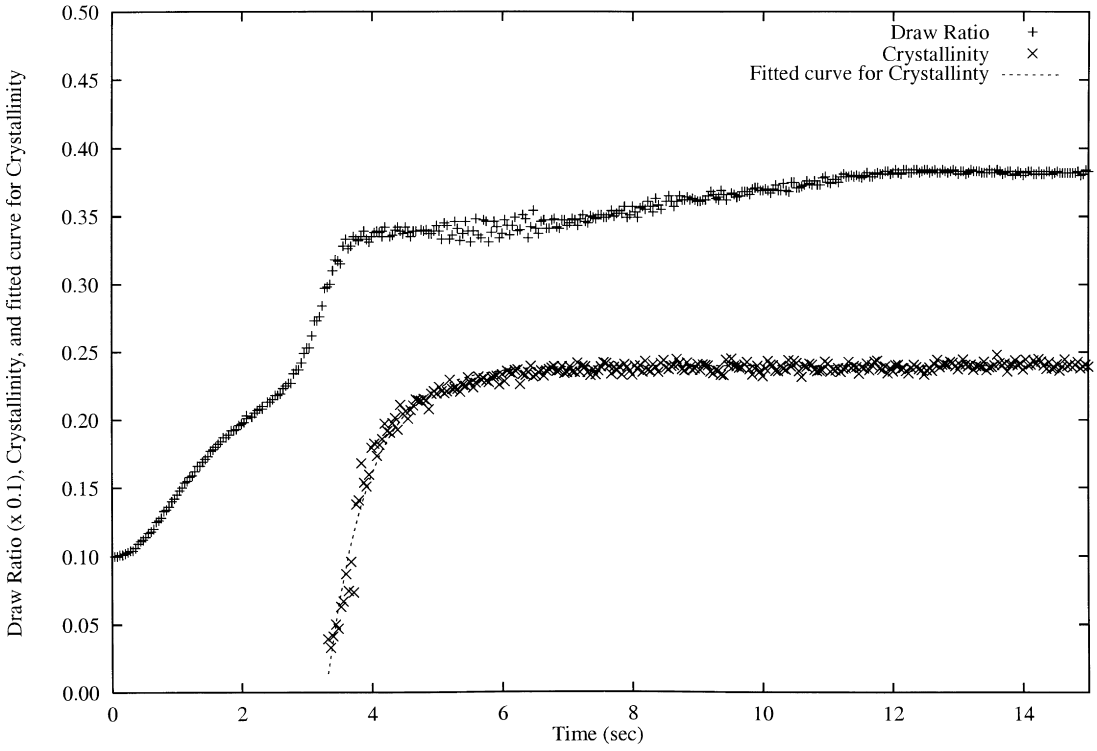

Fig. 6. Plot of the variation in draw ratio (+), crystallinity (×) calculated from the sequence of X-ray diffraction patterns of the PET sample recorded during the drawing at 90°C, draw rate 0.56 s^{-1} and to a final draw ratio 3.8:1. The dotted line indicates the fitted curve based on a first order transformation for the crystallization process.

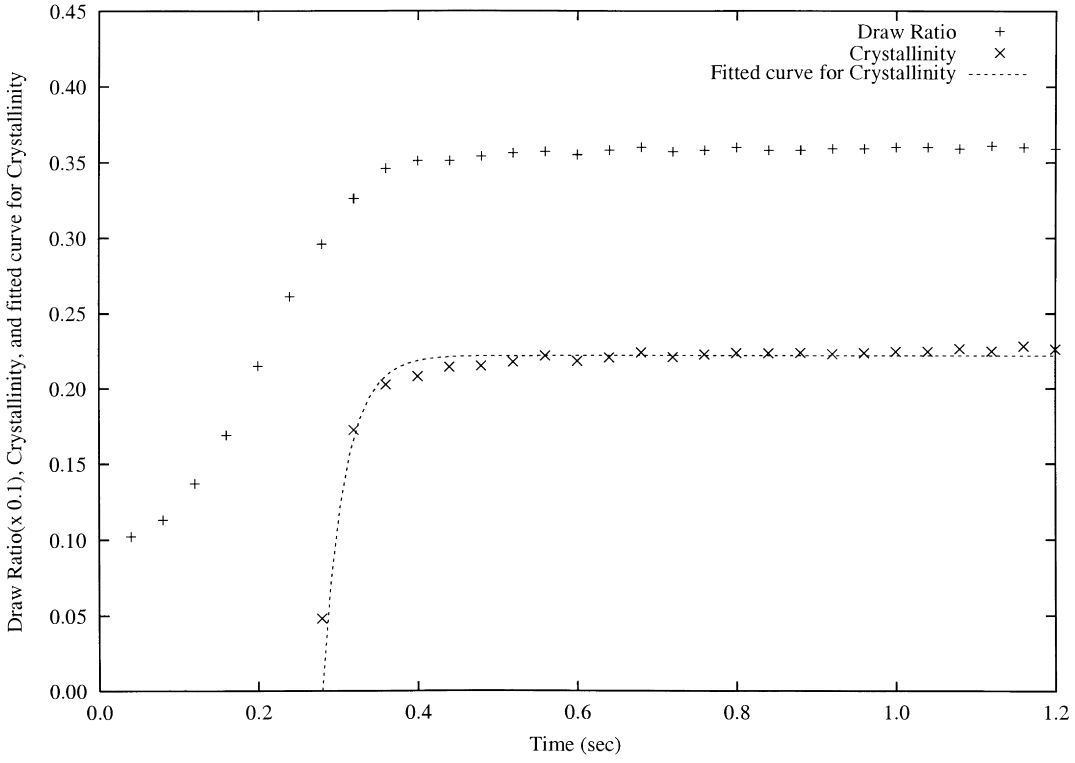

Fig. 7. Plot of the variation in draw ratio (+), crystallinity (×) calculated from the sequence of X-ray diffraction patterns of the PET sample recorded during the drawing at 110°C, draw rate 9.9 s^{-1} and to a final draw ratio 3.6:1. The dotted line indicates the fitted curve based on a first order transformation for the crystallization process.

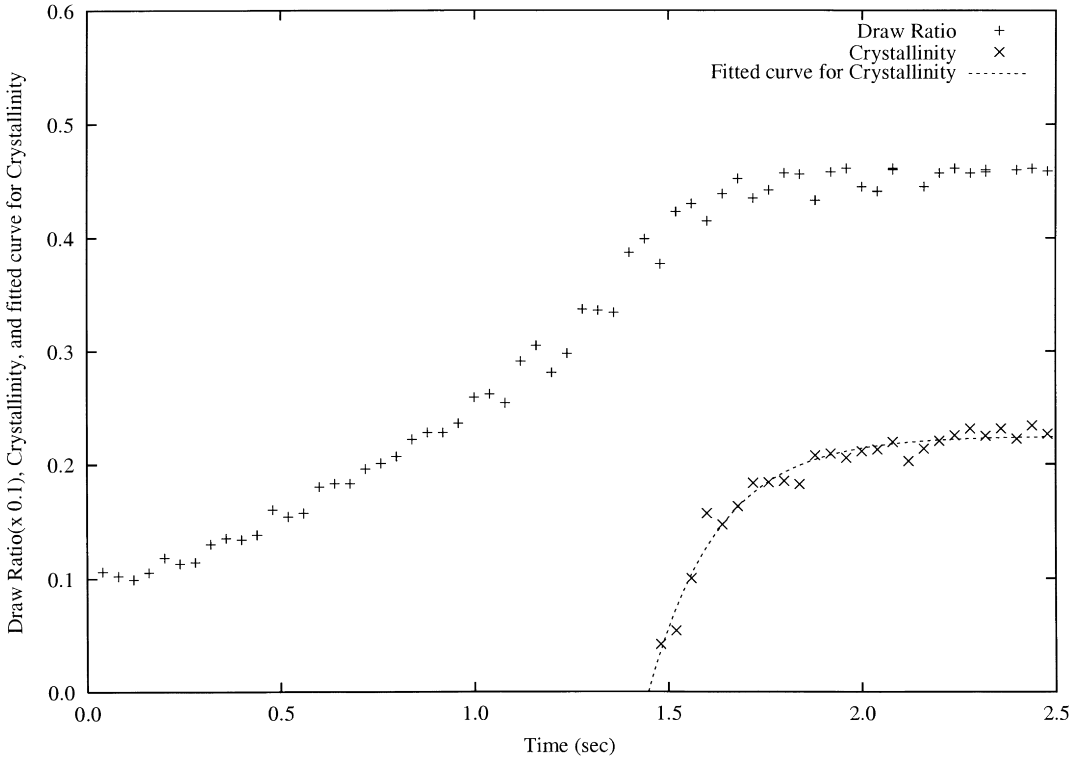

Fig. 8. Plot of the variation in draw ratio (+), crystallinity (×) calculated from the sequence of X-ray diffraction patterns of the PET sample recorded during the drawing at 110°C, draw rate 2.1 s^{-1} and to a final draw ratio 4.6:1. The dotted line indicates the fitted curve based on a first order transformation for the crystallization process.

of drawing at a point close to a draw ratio of 3.0:1. There is some evidence in this case that the kinetics are deviating from the first order transformation process. Attempts have been made to fit the data to generalised Avrami kinetics but it has not been possible to obtain linear behaviour in the standard analysis plots. The final crystalline diffraction is similar to the pattern at the faster draw rate in Fig. 1 but more diffuse in appearance, indicating that the crystal orientation and texture are less well defined.

For Figs. 3 and 7, the draw temperature is higher at 110°C with a draw rate of 9.9 s^{-1} and a final draw ratio of 3.6:1. In view of the higher mobility at 110°C, this case is also expected to be in the regime where chain retraction can occur during the deformation process [4]. The higher draw rate and crystallization rate in this case makes it difficult to resolve the sequence of events in individual frames. In frame 9 at 0.36 s in Fig. 3c, there is already a well-resolved crystal diffraction pattern. However, in a previous frame 7 (Fig. 3b) at 0.28 s where the draw ratio is only 3.0: 1, the pattern is dominated by diffuse scattering and a crystalline component is difficult to resolve. It is, however, possible to discern faint features associated with the crystalline pattern but at an estimated crystallinity of 5%. Hence despite the poor time resolution there is evidence of crystallization starting during the drawing. The crystalline pattern that develops in this case has a different character to Figs. 1 and 2. The relative intensities of the crystal reflection are now closer to that expected with uniaxial symmetry and now show a relatively intense (100) reflections, which were difficult to resolve in Fig. 1. However, there is a further detectable difference in that there are vertical shifts of reflections relative to the layerlines indicating a tilt of the *c*-axis of the crystals relative to the orientation axis. This displacement is particularly clear for the (100) reflections and becomes progressively more pronounced as the draw temperature is increased.

For Figs. 4 and 8, the draw temperature is at 110°C but with a lower draw rate of 2.1 s^{-1} and a final draw ratio of 4.6:1. There is now no dispute that the crystallization starts during the drawing stage at a draw ratio below 4:1. The tilt of the crystalline pattern relative to the orientation axis is now more pronounced than in Fig. 3 indicating that the degree of tilting also depends on the drawing rate.

Table 1 lists some of the key parameters derived from the data for a range of selected drawing conditions; these include:

(i) The mean draw rate up to the onset of crystallization;
(ii) The draw ratio and the orientation parameter, $\langle P_2(\cos\theta)\rangle$, at the onset of crystallization; and
(iii) The crystallization rate constant k_c.

For simplicity the rate constant, k_c, has been derived on the basis of the first order transformation process, even in those

Table 1
Drawing and crystallization behaviour for experiments covering a range of temperature and draw rates

Temperature (°C)	Draw rate (s^{-1})	$\langle P_2(\cos\theta)\rangle$ at the onset point	Crystallization Rate k_c (s^{-1})	Draw ratio at onset of crystallization	Final draw ratio
90	12.8	0.47	10.6	3.7	3.7
90	3.5	0.28	5.2	3.2	3.2
90	0.56	0.22	1.5	3.0	3.8
100	6.6	0.18	7.5	2.5	2.9
100	3.2	0.18	9.6	2.6	3.5
100	2.5	0.16	5.2	2.7	3.8
110	10.3	0.13	40	3.5	3.8
110	2.1	0.08	2.4	4.0	4.6
110	3.0	0.08	6.2	3.0	4.6
120	12.2	0.07	24	4.4	4.6
120	11.4	0.04	2.1	2.2	2.9
120	3.4	–	None	–	5.8

cases such as Fig. 6 where there is evidence of a deviation in behaviour.

Fig. 9 shows a collation of data from 30 experiments covering a wide range of draw parameters in which k_c is plotted against the orientation parameter $\langle P_2(\cos\theta)\rangle$ of the deformed non-crystalline chains at the onset point of crystallisation. For added clarity, the data points for different draw temperatures have been plotted with different symbols. It is of interest to note that at 120°C and a draw rate of 3.4 s^{-1}, a very low level of orientation is achieved and no oriented crystallisation is observed. This draw rate is comparable with the estimated chain reptation rate at 120°C [4] and is consistent with chains segments disorienting before the oriented crystallization process can occur.

4. Discussion

4.1. Factors effecting crystallization rate

It is well established that the rate of crystallization is very sensitive to the degree of molecular orientation [8]. However, there has so far been little information on the nature of this relationship. The plot in Fig. 9 clearly demonstrates the high sensitivity of the crystallization rate to molecular orientation but it also emphasises the importance of temperature. The plot shows a systematic clustering with respect to draw temperature with each cluster exhibiting a similar underlying trend with respect to orientation but with a vertical shift between data clusters. The trend within each temperature cluster gives a more detailed picture of the quantitative effect of orientation than has been available hitherto.

These results indicate that the apparent insensitivity to temperature from our more limited previous experiments [1,2] was in fact due to the fortuitous choice of drawing conditions used in these experiments. The apparent insensitivity would appear to have been the consequence of opposing effects of temperature and orientation. Namely that for a given draw ratio an increase in temperature reduces the

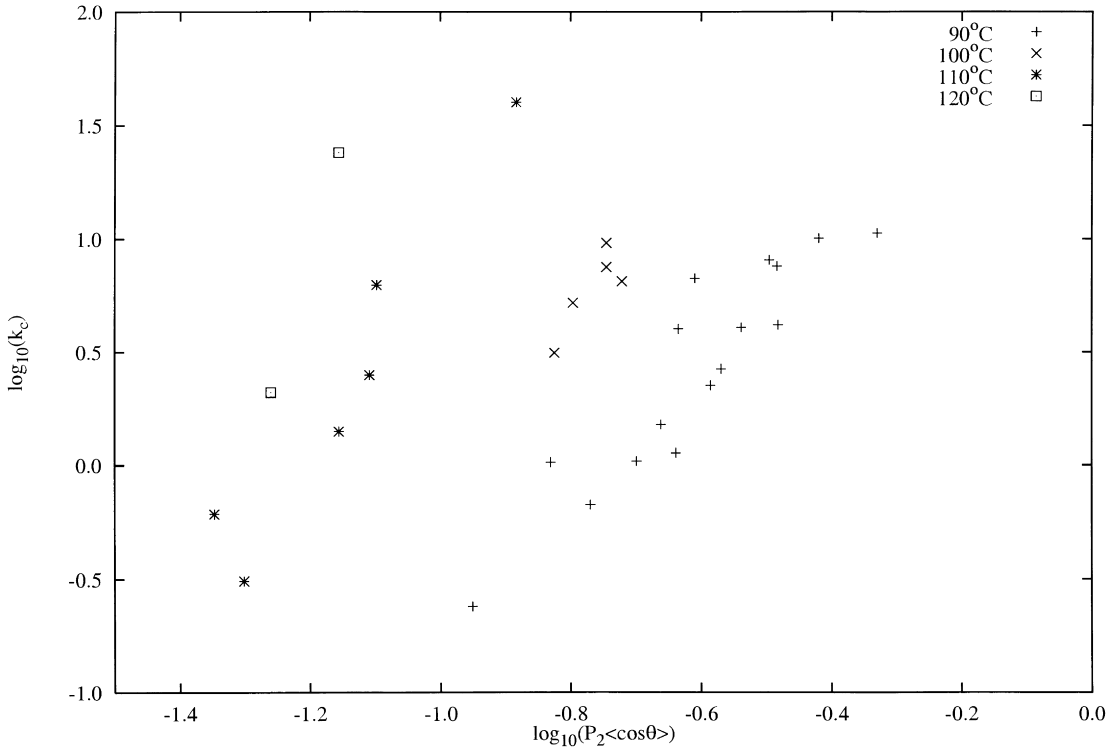

Fig. 9. Logarithm of crystallization rate, k_c versus logarithm of ($\langle P_2(\cos\theta)\rangle$) at the onset of crystallization drawn at 90, 100, 110 and 120°C.

crystallization rate as a result of lower network orientation. This is counteracted by the effects of increased molecular mobility on the crystallization kinetics. Temperature will also affect the thermodynamic drive to crystallization in a corresponding way to its role in normal isotropic crystallization.

If one assumes that the factors affecting the crystallization rate are analogous to those observed in the unoriented state except that there is an additional entropic driving force from the chain orientation, it then becomes feasible to separate the effects of temperature and of orientation. Accordingly one would expect the rate of crystallization of the strain induced crystallization process, k_c, to be represented by a relationship of the form [9,10]:

$$k_c = k_{or} k_{tr} k_n$$

where $k_{or}(\langle P_2(\cos\theta)\rangle)$ represents the relationship with molecular orientation, $k_{tr}(f)$ is the dependence on molecular mobility, $k_n(f)$ is a free energy nucleation term analogous to isotropic crystallization.

Since the drawing experiments are carried out in the region close to the T_g of PET, it is appropriate to propose that the mobility factor, $k_{tr}(f)$, is represented by a WLF transport relationship. Le Bourvellec has determined a suitable WLF relationship for PET with the following parameters based on a reference temperature of 84.2°C [4,11]:

$$\log_{10} a_T = (\log_{10} k_{tr}) = \frac{8.4(T - 84.2)}{42.4 + T - 84.2}$$

where T is temperature in °C.

In their studies of the isotropic crystallization kinetics of PET, both Palys and Phillips [9] and van Antwerpen and van Krevelen [10] found their results could be correlated with a free energy nucleation term of the form:

$$k_n = \exp\left(-\frac{AT_m^2}{T^2(T_m - T)}\right)$$

where A depends on specific polymer parameters and where in this equation T_m and T are absolute temperatures being, respectively, the equilibrium melting temperature and the crystallization temperature. Although there is a basis for using this relationship for analysing the linear growth rate of crystalline lamellae in spherulites grown from an isotropic PET melt, it is questionable whether the mechanism of such crystal growth is appropriate for the crystalline entities developing from an oriented chain network. There are also concerns with extrapolating such a relationship to the very high supercooling in the temperature range of the current drawing experiments. From a comparison of the two temperature dependent terms, the effect on the crystallization rate of changing temperature in the range 90–120°C is dominated by the transport term k_{tr}. Using parameters suggested by Palys and Phillips for k_n indicates that the variation in k_n is minor in our range of interest. In view of this k_n has been ignored in what follows.

Accordingly, the above expressions suggest that the form of k_{or} can be derived from the measured k_c using the following logarithmic relationship to eliminate the effects due to temperature:

$$\log k_{or} = \log k_c - \log a_T.$$

Fig. 10 shows the result of using this relationship on the data in Fig. 9 to shift the measured data to a reference temperature of 90°C. Although there is still a degree of scatter in these shifted data, the new plot does reveal the nature of an underlying relationship which can be regarded as the master curve showing the effect of orientation on k_c for any particular temperature. The data points on this log–log plot cluster around a linear relationship with a slope close to four, inferring that in the range of the experimental conditions that have been examined there is an underlying temperature independent relationship of the form:

$$k_c = \text{constant}(\langle P_2(\cos\theta)\rangle)^n \text{ where } n \sim 4.$$

The temperature-shifting device used for Fig. 10 relates data from temperature ranges with different regimes of chain relaxation. For example, above about 100°C, significant chain retraction occurs during the time scale of the deformation, whereas at 90°C there will be minimal slippage of chains through entanglements during the deformation stage. At 120°C, significant chain reptation is expected to occur. It should be noted that Fig. 10 is a hypothetical plot for a 90°C reference temperature. It does not necessarily indicate that all points of the plot can be accessed in a practical drawing experiment at 90°C since it does not take account of the concurrent chain relaxation. For instance in the region of lower $\langle P_2(\cos\theta)\rangle$ values, it is plausible that at 90°C the chains will relax to isotropic configurations faster than the indicated crystallization rate and that, therefore, oriented crystallization will be precluded.

4.2. Effects of relaxation on crystal orientation

The tilting of the crystals relative to the drawing axis, which is indicated by the splitting of ($hk0$) reflections about the equator, increases with both increasing temperature and decreasing draw rate.

The type of crystal tilting appears to be the same as the effect documented by Daubeny et al. [12], Bonart [13] and Asano and Seto [14] in annealed PET fibres. Daubeny et al. [12] deduced that the crystal chain axis was tilting within the (−230) plane. They were unable to ascribe a simple explanation for this specific behaviour but presumed it was related to the way the triclinic structure of the PET cell interacted with the surrounding chain network. Asano and Seto [14] proposed that more than one mechanism was responsible, depending on temperature. In all these studies tilted crystals were obtained by post annealing predrawn, well aligned fibres at temperatures up to 250°C. This contrasts with the present drawing experiments, where the tilted crystals are formed directly from a non-crystalline

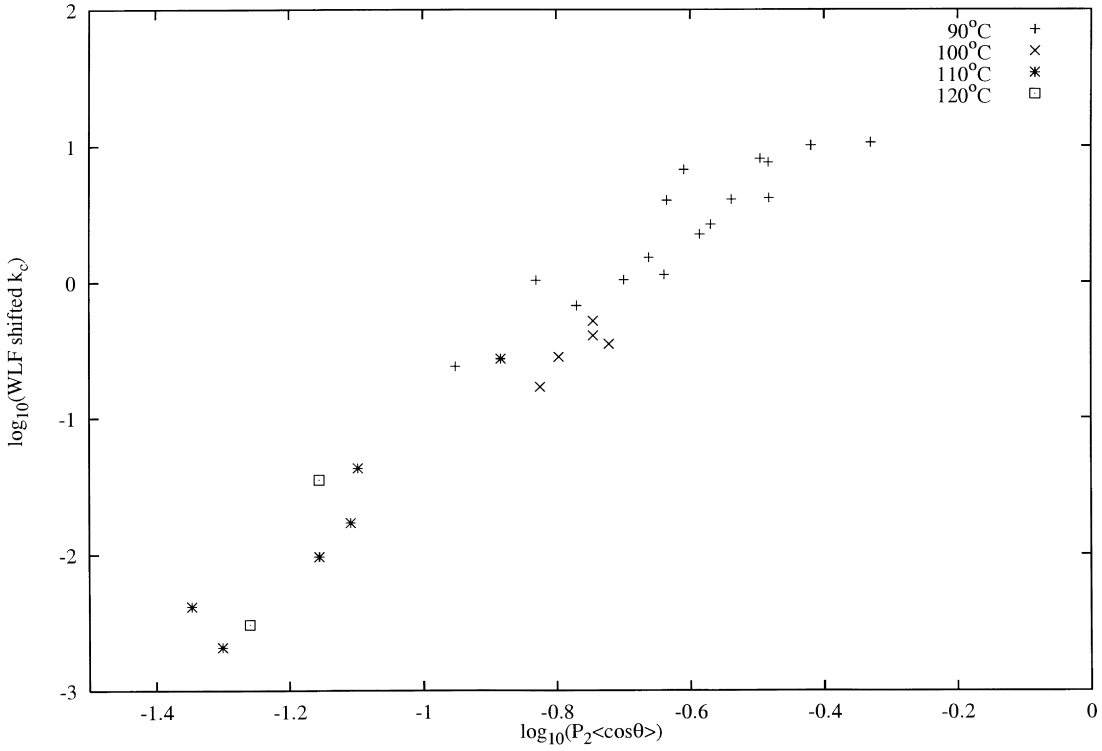

Fig. 10. Logarithm of crystallization rates shifted with WLF relationship for a reference temperature of 90°C versus logarithm of ($\langle P_2(\cos\theta)\rangle$) at the onset of crystallization.

network. Comparison of successive diffraction patterns in each experiment shows that there is little change in the tilt and distribution of the crystallites throughout the period of observation. This indicates that the tilt of the evolving crystallite population is mostly determined by the orientation of the nuclei rather than by subsequent relaxation of the crystallites as was observed in the experiments of Daubeny et al. [12]. It suggests that the orientation of the crystal nuclei depends on the molecular orientation at the onset of crystallization. The observed dependence of crystallite tilt on both temperature and draw rate suggests that the orientation of the seed nuclei may be influenced by the network relaxation processes.

4.3. Identification of three regimes for PET deformation

Fig. 11 shows a schematic map of the estimated relaxation rates of the retraction and reptation processes discussed in our previous paper [4]. The shift in the relaxation rates with temperature have been calculated from the above WLF relationship suggested by Le Bourvellec [11]. Three regimes of behaviour are discernible on the map. In Regime I, the draw rate is faster than the chain retraction rate $1/\tau_B$. This is the regime where the development of $\langle P_2(\cos\theta)\rangle$ was found to be relatively insensitive to draw rate and where the onset of crystallization is delayed until the end of the deformation process [4]. The (*hk*0) reflections of the diffraction patterns are found in these cases to be close to the equator indicating that the crystal chain axes are well oriented with respect to the draw direction. In Regime II, the draw rate is intermediate between the retraction rate, $1/\tau_B$, and the chain reptation rate, $1/\tau_C$. This is the regime where $\langle P_2(\cos\theta)\rangle$ was found to decrease significantly with draw rate and where there is evidence of the onset of crystallization occurring before the end of the mechanical deformation [4]. The diffraction patterns for these cases show an increasing degree of crystal tilting with increasing temperature and reducing draw rate. Finally, Regime III is associated with draw rates slower than chain reptation. No significant segment orientation is achieved during the deformation stage in this regime and oriented crystallization is not observed.

According to the concepts developed by Doi and Edwards [15] and de Gennes [16], deformed chains in Regime II will have the freedom to retract within an enclosing tube to recover their curvilinear length. It is presumed that the crystal nuclei with the triclinic PET structure will interact with the surrounding deformed network in a similar way to that suggested by Daubeny et al. and adopt a tilt depending on the forces exerted by the network. The absence of a significant tilt in Regime I would appear to be related to the lack of freedom of the network chain to retract through entanglements resulting in more chain strands that are highly aligned in the draw direction. The crystal nuclei forming within these network constraints are more likely to be aligned without tilting effects.

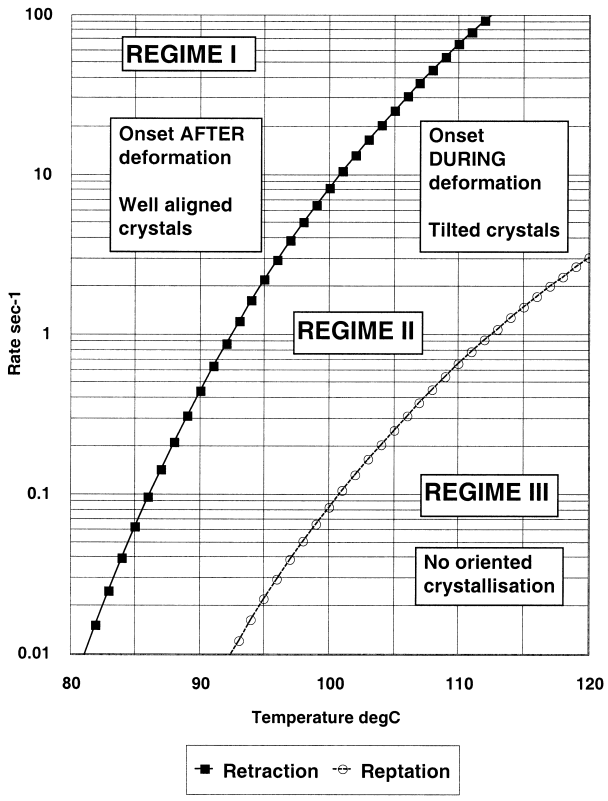

Fig. 11. Schematic map of estimated chain relaxation rates as a function of temperature, illustrating changes in oriented crystallization behaviour.

4.4. Nucleation of oriented crystals

The process of crystal nucleation in Regime I warrants further investigation, particularly with regard to two related issues.

The first is the possibility that a significant alignment of chain segments along the draw direction will encourage the formation of a mesophase during drawing as part of the crystal nucleation process. Keller has pointed out that there is a theoretical justification on thermodynamic grounds for an oriented mesophase being favoured as an intermediate step before crystallization [17]. Diffraction patterns, that have been ascribed to an oriented mesophase, have already been reported from certain highly drawn fibres of PET and poly(ethylene naphthalate) (PEN) [14,18–20]. A key indication of an oriented mesophase is the presence of a sharp meridional reflection combined with the absence of normal crystalline reflections. Recent experiments on PET/PEN copolymers by Welsh et al. [21] have demonstrated that such a mesophase can be a precursor to crystallization during subsequent annealing. The present time-resolved synchrotron experiments provide an opportunity for observing mesophases during the drawing process while the chains are still mobile. Detailed analysis on the most highly drawn samples at 90°C does in fact show evidence of the mesophase reflection developing during the latter stages of the deformation and then being replaced by crystalline order after the drawing has stopped. So far it has not been possible to resolve this reflection in samples drawn at higher temperatures and slower rates. Details of this transient mesophase behaviour have been reported separately [22].

The second issue of interest is the mechanism of the nucleation process and the associated kinetics. Imai et al. [23] have used SAXS and WAXS to study the nucleation process in unoriented PET at temperatures just above the T_g and have proposed a model involving the evolution of density fluctuations. Terril et al. [24] have proposed a similar mechanism in their synchrotron studies of both unoriented and oriented polypropylene. Imai et al. [23] identified an induction period before crystallization in which there was a change in the SAXS profile. This was ascribed to the evolution of density fluctuations via a spinodal decomposition process in which rod like configurations segregated from more random chain configurations. It was proposed that crystal nucleation does not occur until the rod -like configurations reach a critical size. A mechanism for this spinodal-assisted nucleation has recently been proposed by Olmsted et al. [25].

In the case of crystallization from the oriented state, Strobl [26] has reported observations on pre-oriented amorphous PET when it is heated just above T_g. He interpreted SAXS data in terms of a spinodal mechanism in which there is a continuous growth in amplitude and order of density fluctuations throughout the crystallization process to the final extent of crystalline order. He did not separate out an induction period and showed that the whole process was consistent with spinodal decomposition. Strobl's experimental situation is closer to the present case with the important exception that our synchrotron experiments monitor the whole drawing and crystallization process at one temperature.

The present experiments provide an opportunity to characterise the full sequence of events and their timescales. Therefore, in addition to the observation of a transient mesophase behaviour for certain conditions, it is also possible to monitor the development of a crystalline phase. An analysis of these synchrotron data indicate that during the crystallization process the crystalline reflections grow in amplitude but with no significant change in half width thus implying little change in perfection or size of crystallites. Fig. 12 shows an example of the variation of the area and halfwidth of the (010) crystalline reflection during the development of the crystallinity for one set of data. There is only a slight decrease in width (indicating an increase in perfection or size) after much longer times as part of a secondary, annealing process [1]. This indicates that the primary crystallization kinetics are associated with an increase in the number or amount of crystals rather than crystallization by evolution of density variations as proposed by Strobl [26]. As has been pointed out previously [1,2] the apparent first order transformation of the primary crystallization process is consistent with the sporadic nucleation of crystals in which the transformation rate is

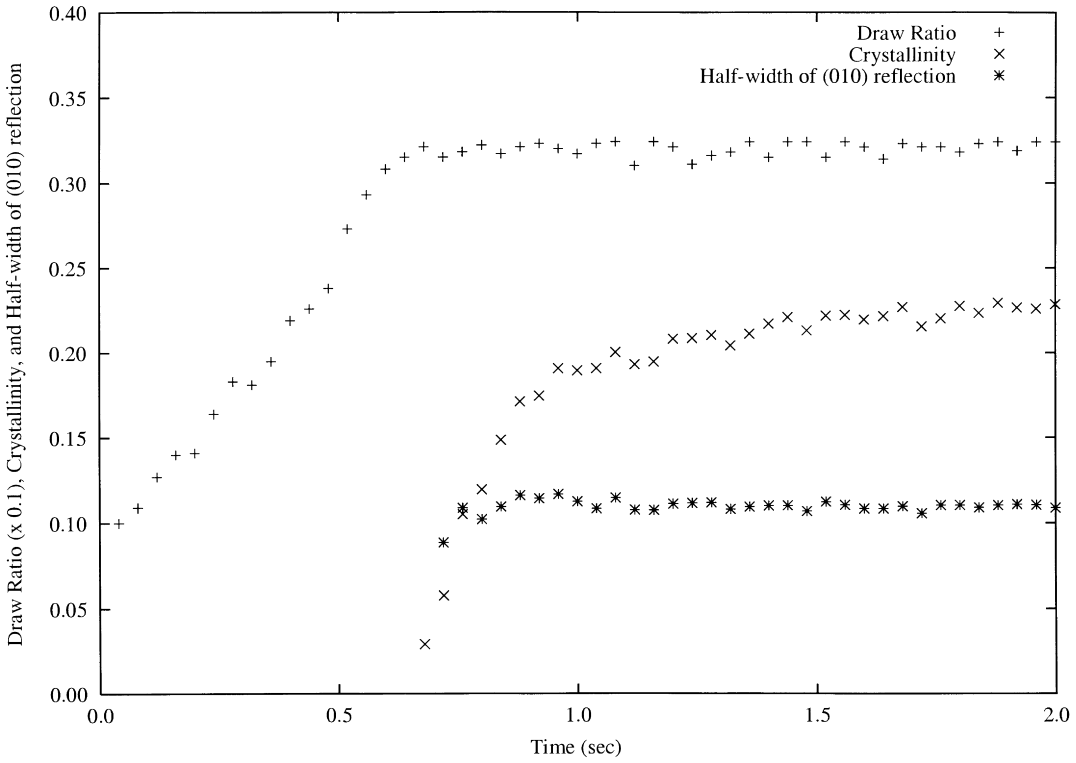

Fig. 12. Development of area and half-width, in arbitrary units, of the (010) crystal reflection for a sample drawn at 90°C and a draw rate 3.5 s^{-1} to a final draw ratio 3.2:1. Also shown is the development of the draw ratio.

proportional to the amount of remaining, unnucleated regions.

It is conceivable that the sporadically forming crystals originate from oriented density fluctuations that are analogous to those observed by Imai et al. [23] in isotropic PET during the induction period and that these fluctuations are associated with the observed mesophase diffraction. In this case the evolution of the fluctuations to form rod-like configurations will be assisted by the imposed alignment in the draw direction. The observed dependence in Fig. 10 of the rate of crystallization on the segment orientation $\langle P_2(\cos\theta)\rangle$ would then be expected to be related to the amount and nature of mesophase regions created.

In this connection, it should be noted that the approximate fourth power dependence on $\langle P_2(\cos\theta)\rangle$ is based on the overall trend of the data in Fig. 10 and is taken from experiments covering a range of draw rates encompassing all the main chain relaxation processes. In the region associated with Regime I where the mesophase characteristics are detectable, there is a suggestion that the trend may be reducing in slope, thus reducing the sensitivity to $\langle P_2(\cos\theta)\rangle$ in this regime.

5. Conclusions

The observed crystalline diffraction patterns indicate that the orientation texture of the developing crystals depends on the relation of the drawing conditions to the chain relaxation processes which were identified previously [4]. For the regime of faster draw rates and lower draw temperature, where the drawing rate is faster than the chain retraction process and where the onset of crystallization is delayed until the end of drawing, the crystal chain axes are well aligned along the draw direction. There is, however, a tendency for preferred alignment of (100) plane in the plane of the sample. At higher temperatures and at draw rates slower than chain retraction where the crystallization onset occurs during drawing, there is an increasing tilt of the crystal chain axis away from the draw direction. At even high temperatures and slower draw rates, where the draw rates become comparable with chain reptation, no orientated crystallization was observable. Irrespective of the drawing regime, the crystal orientation texture remains essentially unaltered over the whole crystallization process and appears to be related to the orientation adopted by the original crystal nuclei. It is also observed that the halfwidth of the crystalline reflection remains essentially unchanged during the crystallization process. These observations are relevant to an understanding of the mode of nucleation and growth of the crystalline phase.

With the availability of data from a wider range of draw conditions it has now been shown that the insensitivity of crystallization rate to temperature that was reported previously [1,2] is the result of opposing factors. For a given degree of segment orientation, there is a strong

dependence of crystallization rate on temperature due to the increased segment mobility at higher temperatures. However, the enhanced mobility also increases chain relaxation and results in a lower degree of segment orientation for a given draw ratio. When the segment mobility effect is factored out by shifting the crystallization rate with a WLF factor, the overall trend of the crystallization rates for all drawing regimes follow an underlying fourth power dependence on the value of $\langle P_2(\cos\theta)\rangle$ at the crystallization onset. In the region of Regime I, where the draw rate is believed to be fast compared with chain retraction and where there is evidence of a transient mesophase, the dependence on $\langle P_2(\cos\theta)\rangle$ may be less marked.

Acknowledgements

We wish to thank Prof. Lucien Monnerie for valuable discussions, particularly on the influence of chain relaxation processes. This work was supported by the allocation of beam time at the ESRF. We are grateful to M. Daniels, M.G. Davies, G. Dudley, E.J.T. Greasley, G. Marsh, M. Wallace and C. Sutton for technical support and help with preparation of the manuscript.

References

[1] Blundell DJ, MacKerron DH, Fuller W, Mahendrasingam A, Martin C, Oldman RJ, Rule RJ, Riekel C. Polymer 1996;37:3303.
[2] Mahendrasingam A, Martin C, Fuller W, Blundell DJ, Oldman RJ, Harvie JL, Mackerron DH, Riekel C, Engstrom P. Polymer 1999;40:5553.
[3] Blundell DJ, Oldman RJ, Fuller W, Mahendrasingam A, Martin C, MacKerron DH, Harvie JLRJ, Riekel C. Polym Bull 1999;42:357.
[4] Blundell DJ, Mahendrasingam A, Martin C, Fuller W, Mackerron DH, Harvie JL, Oldman RJ, Riekel C. Polymer 2000;41:7793.
[5] Salem DR. Polymer 1992;33:3182.
[6] Casey K. Polymer 1977;18:1219.
[7] Bower DI, Jarvis DA, Ward IM. J Polym Sci-Phys 1986;24:1459.
[8] Smith FS, Steward RD. Polymer 1974;15:283.
[9] Palys LH, Phillips PJ. J Polym Sci-Phys 1980;18:829.
[10] Van Antwerpen F, Van Krevelen DW. J Polym Sci-Phys 1972;10:2423.
[11] Le Bourvellec G. Thesis Doct. Ing., Universite Paris VI, 1984.
[12] Daubeny RdeP, Bunn CW, Brown CJ. Proc R Soc A 1954;226:531.
[13] Bonart R. Kolloid-Z 1966;213:1.
[14] Asano T, Seto T. Polym J 1973;5:72.
[15] Doi M, Edwards SF. The theory of polymer dynamics. Oxford: Clarendon Press, 1986.
[16] de Gennes P-G. J Chem Phys 1971;55:572.
[17] Keller A. In: Dosiere M, editor. Crystallization of polymers, NATO advanced research workshop, Mons, Belgium: Kluwer, 1992. p. 1.
[18] Bonart R. Kolloid-Z 1968;231:16.
[19] Jakeways R, Klein JL, Ward IM. Polymer 1996;37:3761.
[20] Carr PL, Nicholson TM, Ward IM. Polym Adv Technol 1997;8:592.
[21] Welsh GE, Blundell DJ, Windle AJ. Macromolecules 1998;31:7562.
[22] Mahendrasingam A, Martin C, Fuller W, Blundell DJ, Oldman RJ, Mackerron DH, Harvie JL, Riekel C. Polymer 2000;41:1217.
[23] Imai M, Kaji K, Kanaya T. Macromolecules 1994;27:7103.
[24] Terril NJ, Fairclough PA, Towns-Andrews E, Komanschek BU, Young RJ, Ryan AJ. Polymer 1998;39:2381.
[25] Olmsted PD, Poon WCK, McLeish TCB, Terril NJ, Ryan AJ. Phys Rev Lett 1998;81:373.
[26] Strobl G. The physics of polymers. 2nd ed.. Berlin: Springer, 1997 (p. 173).